

Zinc–Zinc Bonded Zirconocene Structures. Synthesis and Characterization of $Zn_2(\eta^5-C_5Me_5)_2$ and $Zn_2(\eta^5-C_5Me_4Et)_2$

Abdessamad Grirrane,[†] Irene Resa,[†] Amor Rodriguez,[†] Ernesto Carmona,^{*,†}
Eleuterio Alvarez,[†] Enrique Gutierrez-Puebla,[‡] Angeles Monge,[‡] Agustín Galindo,[§]
Diego del Río,[†] and Richard A. Andersen^{||}

Contribution from the Instituto de Investigaciones Químicas-Departamento de Química Inorgánica, Universidad de Sevilla-Consejo Superior de Investigaciones Científicas, Américo Vespucio 49, 41092 Sevilla, Spain, Instituto de Ciencia de Materiales de Madrid, Consejo Superior de Investigaciones Científicas, Campus de Cantoblanco, 28049 Madrid, Spain, Departamento de Química Inorgánica, Universidad de Sevilla, Apto. 553, 41071 Sevilla, Spain, and Chemistry Department, University of California, Berkeley, California 94720

Received September 21, 2006; E-mail: guzman@us.es

Abstract: While, in general, decamethylzirconocene, $Zn(C_5Me_5)_2$, and other zirconocenes, $Zn(C_5Me_4R)_2$ ($R = H, Bu^t, SiMe_3$), react with dialkyl and diaryl derivatives, ZnR'_2 , to give the half-sandwich compounds $(\eta^5-C_5Me_4R)ZnR'$, under certain conditions the reactions of $Zn(C_5Me_5)_2$ with $ZnEt_2$ or $ZnPh_2$ produce unexpectedly the dizirconocene $Zn_2(\eta^5-C_5Me_5)_2$ (**1**) in low yields, most likely as a result of the coupling of two $(\eta^5-C_5Me_5)Zn^+$ radicals. An improved, large scale (ca. 2 g) synthesis of **1** has been achieved by reduction of equimolar mixtures of $Zn(C_5Me_5)_2$ and $ZnCl_2$ with KH in tetrahydrofuran. The analogous reduction of $Zn(C_5Me_4R)_2$ ($R = H, SiMe_3, Bu^t$) yields only decomposition products, but the isotopically labeled dimetallocene $^{68}Zn_2(\eta^5-C_5Me_5)_2$ and the related compound $Zn_2(\eta^5-C_5Me_4Et)_2$ (**2**) have been obtained by this procedure. Compound **2** has lower thermal stability than **1**, but it has been unequivocally characterized by low-temperature X-ray diffraction studies. As for **1** a combination of structural characterization techniques has provided unambiguous evidence for its formulation as the Zn–Zn bonded dimer $Zn_2(\eta^5-C_5Me_4Et)_2$, with a short Zn–Zn bond of 2.295(3) Å indicative of a strong Zn–Zn bonding interaction. The electronic structure and the bonding properties of **1** and those of related dizirconocenes $Zn_2(\eta^5-Cp)_2$ have been studied by DFT methods (B3LYP level), with computed bond distances and angles for dizirconocene **1** very similar to the experimental values. The Zn–Zn bond is strong (ca. 62 kcal·mol⁻¹ for **1**) and resides in the HOMO-4, that has a contribution of Zn orbitals close to 60%, consisting mostly of the Zn 4s orbitals (more than 96%).

Introduction

The chemistry of metallocenes continues to attract a great deal of attention^{1–4} due to their successful applications in many areas of chemistry such as olefin polymerization catalysis,⁵ asymmetric catalysis,⁶ C–H bond activation,⁷ or bioorganometallic

chemistry.⁸ The use of substituted, bulky cyclopentadienyl ligands⁹ has permitted the discovery of new, unexpected structures in mono- and polynuclear metallocenes of both the transition (d and f) and the main group elements. Figure 1 shows structural types (a–e) found for divalent metallocenes, MCP^2 . However, despite initial expectations,¹⁰ binuclear metallocenes of structure f (Figure 1), where a pair of directly bonded metal atoms unsupported by bridging ligands are sandwiched between two cyclopentadienyl rings whose planes are essentially per-

[†] Universidad de Sevilla-Consejo Superior de Investigaciones Científicas.

[‡] Campus de Cantoblanco.

[§] Departamento de Química Inorgánica, Universidad de Sevilla.

^{||} University of California.

- (1) (a) Kealy, T. J.; Pauson, P. L. *Nature* **1951**, *168*, 1039. (b) Miller, S. A.; Tebboth, J. A.; Tremaine, J. F. *J. Chem. Soc.* **1952**, 633.
- (2) (a) Fischer, E. O.; Pfab, W. *Z. Naturforsch.* **1952**, *7b*, 377. (b) Wilkinson, G.; Rosenblum, M.; Whiting, M. C.; Woodward, R. B. *J. Am. Chem. Soc.* **1952**, *74*, 2125. (c) Wilkinson, G. *J. Am. Chem. Soc.* **1952**, *74*, 6146.
- (3) Jutzi, P.; Burdford, N. In *Metallocenes*; Togni, A., Halterman, R. L., Eds.; Wiley: New York, 1998; Vol. 1, Chapter 1.
- (4) For example, see: (a) Yamamoto, A. *J. Organomet. Chem.* **2000**, *600*, 159. (b) Pauson, P. L. *J. Organomet. Chem.* **2001**, *637–639*, 3. (c) Fischer, E. O.; Jira, R. *J. Organomet. Chem.* **2001**, *637–639*, 7. (d) Rosenblum, M. *J. Organomet. Chem.* **2001**, *637–639*, 13. (e) Whiting, M. C. *J. Organomet. Chem.* **2001**, *637–639*, 16. (f) Cotton, F. A. *J. Organomet. Chem.* **2001**, *637–639*, 18.
- (5) *Metallocene-Based Polyolefins*; Scheirs, J., Kaminsky, W., Eds.; John Wiley & Sons Ltd., Chichester, 2000; Vols. 1 and 2.
- (6) *Ferrocenes*; Togni, A., Hayashi, T., Eds.; Verlag Chemie: Weinheim, 1995.

- (7) For some illustrative examples, see: (a) Arndtsen, B. A.; Bergman, R. G. *Science* **1995**, *270*, 1970. (b) Chen, H.; Schlecht, S.; Semple, T. C.; Hartwig, J. F. *Science* **2000**, *287*, 1995. (c) Pamplin, C. B.; Legzdins, P. *Acc. Chem. Res.* **2003**, *36*, 223. (d) Jones, W. D. *Inorg. Chem.* **2005**, *44*, 4475.
- (8) Jaouen, G.; Top, S.; Vessières, A.; Alberto, R. *J. Organomet. Chem.* **2000**, *600*, 23.
- (9) (a) Jutzi, P.; Burdford, N. *Chem. Rev.* **1999**, *99*, 969. (b) Janiak, C.; Schumann, H. *Adv. Organomet. Chem.* **1991**, *23*, 291. (c) Hays, M. L.; Hanusa, T. P. *Adv. Organomet. Chem.* **1996**, *40*, 117.
- (10) (a) Schneider, J. J.; Godard, R.; Werner, S.; Krüger, C. *Angew. Chem., Int. Ed. Engl.* **1991**, *30*, 1124. (b) Abrahamson, H. B.; Niccolai, G. P.; Heinekey, D. M.; Casey, C. P.; Burstein, B. *Angew. Chem., Int. Ed. Engl.* **1992**, *31*, 471. (c) Kersten, J. L.; Rheingold, A. L.; Theopold, K. H.; Casey, C. P.; Widenhofer, R. A.; Hop, C. E. C. A. *Angew. Chem., Int. Ed. Engl.* **1992**, *31*, 1341. (d) Lutz, F.; Ban, R.; Wu, P.; Koetzle, T. F.; Krüger, C.; Schneider, J. *J. Inorg. Chem.* **1996**, *35*, 2698.

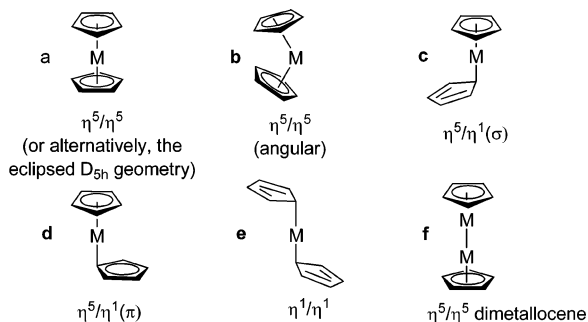


Figure 1. Structural types for divalent metallocenes.

pendicular to the metal–metal bond axis, have remained unknown until recently.

The capacity of metal atoms to form homonuclear (or heteronuclear) metal–metal bonds have given rise to the development of one of the most important areas of modern metal chemistry, e.g., that of metal clusters.¹¹ This ability changes considerably along the Periodic Table not only from one group to another but also for elements of the same group. For instance, one of the most remarkable and distinct features of the group 12 elements, Zn, Cd, and Hg, is their varying tendency to form dinuclear compounds containing $[M-M]^{2+}$ units. Thus, for the heaviest element, mercury, stable diatomic species are known in solution and in the solid state,¹² whereas for zinc and cadmium the almost invariable oxidation state is +2, in the form of mononuclear M^{2+} ions.¹² Only a few exceptions to this rule are known. The dication Cd_2^{2+} has been known for many years, and it has been structurally characterized by X-ray methods in $Cd_2(AlCl_4)_2$ ¹³ and by ¹¹³Cd NMR spectroscopy¹⁴ in $Cd_2Tp^{Me_2}$ (Tp^{Me_2} = hydrotris(3,5-dimethylpyrazolyl)borate). There is evidence for the formation of Zn_2^{2+} ions in $ZnCl_2/Zn$ glasses at high temperatures¹⁵ and in zeolite matrices.¹⁶ The dihydride Zn_2H_2 has been isolated in argon matrices and characterized by vibrational spectroscopy, deuterium substitution, and MP2 calculations.¹⁷ Recently, the formation of mononuclear, para-

magnetic Zn^+ in a microporous crystalline silicoaluminophosphate has been reported.¹⁸

Organozinc compounds are of historical significance,¹⁹ with Frankland's synthesis of $ZnMe_2$ and $ZnEt_2$, the first binary metal alkyls, paving the way for the development of alkyl derivatives of the main group metals and for their countless applications in organic synthesis. In recent years, organozinc compounds have become essential reagents for organic synthesis,²⁰ but despite extensive research, molecular complexes of the metal–metal bonded Zn_2^{2+} unit remain elusive, although the divalent zincocenes, $ZnCp'_2$, form a well-known family of metallocenes with the distinct $\eta^5/\eta^1(\pi)$ structure (**d** in Figure 1).²¹ We have recently communicated the synthesis and structural and electronic properties of $Zn_2(\eta^5-C_5Me_5)_2$, **1**, the first stable molecular compound of zinc with a zinc–zinc bond.²² This report attracted the interest of the scientific community²³ and was followed shortly by a number of theoretical studies dedicated to **1** and also to related species.^{24,25} Furthermore two new examples of zinc–zinc bonded compounds have been provided. Robinson and co-workers have reported the generation²⁶ of $Zn_2[HC-(CMeNAr)_2]_2$ ($Ar = 2,6-Pr^i_2C_6H_3$), with three-coordinate zinc atoms (bidentate β -diketiminate ligands), and very recently Power and co-workers have characterized²⁷ the zinc–zinc bonded species Zn_2Ar_2 for $Ar=C_6H_3-2,6-(C_6H_3-2,6-Pr^i_2)_2$, where the Zn_2^{2+} unit is supported by monodentate ligands. The two compounds have essentially identical Zn–Zn bond lengths of ca. 2.36 Å, approximately 0.05 Å longer than **1**, despite their lower metal coordination number.

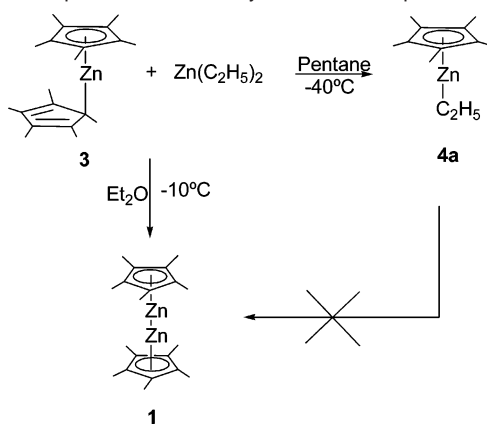
Aware of the importance of our initial report, we have focused our efforts on the synthesis, reactivity, structural properties, and electronic characteristics of dizincocenes and have succeeded recently in isolating and characterizing by X-ray crystallography a second example of a dimetallozene, namely $Zn_2(\eta^5-C_5Me_4Et)_2$, **2**, which features a Zn–Zn bond length of ca. 2.30 Å, practically identical to that of **1**. In this paper we present full details of the work that has allowed their generation and structural characterization, as well as our own study of their electronic structure and bonding properties.

Results and Discussion

$Zn_2(\eta^5-C_5Me_5)_2$ (1**) and $Zn_2(\eta^5-C_5Me_4Et)_2$ (**2**). Synthesis and Reactivity.** During the course of our work on different zincocenes, e.g., $Zn(C_5Me_4SiMe_3)_2$ and related compounds,²⁸

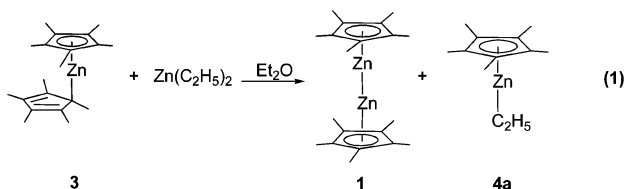
- (11) (a) Cotton, F. A.; Walton, R. A. *Multiple Bonds Between Metal Atoms*, 2nd ed.; Oxford University Press: Oxford, 1993. (b) Schnöckel, H. *J. Chem. Soc., Dalton Trans.* **2005**, 3131.
- (12) (a) Cotton, F. A.; Wilkinson, G.; Murillo, C. A.; Bochmann, M. *Advanced Inorganic Chemistry*, 6th ed.; Wiley: New York, 1999; Chapter 15. (b) Wiberg, N., Ed. *Holleman-Wiberg Inorganic Chemistry*, 34 ed.; Academic Press: New York, 2001; Chapter XXIII.
- (13) (a) Faggiani, R.; Gillespie, R. J.; Vekris, J. E. *J. Chem. Soc., Chem. Commun.* **1986**, 517. (b) Staffel, T.; Meyer, G. Z. *Anorg. Allg. Chem.* **1987**, 548, 45.
- (14) Reger, D. L.; Mason, S. S. *J. Am. Chem. Soc.* **1993**, 115, 10406.
- (15) Kerridge, D. H.; Tariq, S. A. *J. Chem. Soc. A* **1967**, 1122.
- (16) (a) Rittner, F.; Seidel, A.; Boddenberg, B. *Microporous Mesoporous Mater.* **1998**, 24, 127. (b) Seff, K.; Zhen, S.; Bae, D. *J. Phys. Chem. B* **2000**, 104, 515.
- (17) (a) Greene, T. M.; Brown, W.; Andrews, L.; Downs, A. J.; Chertihin, G. V.; Runeberg, N.; Pyykkö, P. *J. Phys. Chem.* **1995**, 99, 7925. (b) Wang, X.; Andrews, L. *J. Phys. Chem. A* **2004**, 108, 11006.
- (18) Tian, Y.; Li, G. D.; Chen, J. S. *J. Am. Chem. Soc.* **2003**, 125, 6622.
- (19) (a) Frankland, E. *Ann.* **1849**, 71, 213. (b) Frankland, E. *J. Chem. Soc.* **1850**, 2, 297. (c) Seyferth, D. *Organometallics* **2001**, 20, 2940.
- (20) *Organozinc Reagents*; Knochel, P., Jones, P., Eds.; Oxford University Press: Oxford, 1999.
- (21) (a) Fischer, E. O.; Hoffmann, H. P.; Treiber, A. Z. *Naturforsch.* **1959**, 14b, 599. (b) Blom, R.; Boersma, J.; Budzelaar, P. H. M.; Fischer, B.; Haaland, A.; Volden, H. V.; Weidlein, J. *Acta Chem. Scand.* **1986**, A40, 113. (c) Fischer, B.; Wijkens, P.; Boersma, J.; van Koten, G.; Smeets, W. J. J.; Spek, A. L.; Budzelaar, P. H. M. *J. Organomet. Chem.* **1989**, 376, 223. (d) Burkey, D. J.; Hanusa, T. P. *J. Organomet. Chem.* **1996**, 512, 165. (e) Budzelaar, P. H. M.; Boersma, J.; van der Kerk, G. J. M.; Spek, A. L.; Duisenberg, A. J. M. *J. Organomet. Chem.* **1985**, 281, 123. (f) Haaland, A.; Samdal, S.; Tverdova, N. V.; Girichev, G. V.; Giricheva, N. I.; Shlykov, S. A.; Garkusha, O. G.; Lokshin, B. V. *J. Organomet. Chem.* **2003**, 684, 351.

- (22) (a) Resa, I.; Carmona, E.; Gutierrez-Puebla, E.; Monge, A. *Science* **2004**, 305, 1136. (b) Del Río, D.; Galindo, A.; Resa, I.; Carmona, E. *Angew. Chem., Int. Ed.* **2005**, 44, 1244.
- (23) (a) Parkin, G. A. *Science* **2004**, 305, 1117. (b) Schnepf, A.; Himmel, H. J. *Angew. Chem., Int. Ed.* **2005**, 44, 3006.
- (24) (a) Xie, Y.; Schaefer, H. F., III; King, R. B. *J. Am. Chem. Soc.* **2005**, 127, 2818. (b) Xie, Y.; Schaefer, H. F., III; Jemmis, E. D. *Chem. Phys. Lett.* **2005**, 402, 414. (c) Timoshkin, A. Y.; Schaefer, H. F. *Organometallics* **2005**, 24, 3343. (d) Liu, Z.-Z.; Tian, W. Q.; Feng, J. K.; Zhang, G.; Li, W.-Q. *THEOCHEM* **2006**, 758, 127. (e) Merino, G.; Beltrán, H. I.; Vela, A. *Inorg. Chem.* **2006**, 45, 1091. (f) Philpott, M. R.; Kawazoe, Y. *Chem. Phys.* **2006**, 327, 283. (g) Pathak, B.; Pandian, S.; Hosmane, N.; Jemmis, E. D. *J. Am. Chem. Soc.* **2006**, 128, 10915.
- (25) (a) Richardson, S. L.; Barnah, T.; Pederson, M. R. *Chem. Phys. Lett.* **2005**, 415, 141. (b) Xie, Z.-Z.; Fang, W.-H. *Chem. Phys. Lett.* **2005**, 404, 212. (c) Kang, H. S. *J. Phys. Chem. A* **2005**, 109, 4342. (d) Kress, J. W. *J. Phys. Chem. A* **2005**, 109, 7757. (e) Zhou, J.; Wang, W.-N.; Fan, K.-N. *Chem. Phys. Lett.* **2006**, 424, 247. (f) Liu Z.-Z.; Tian, W. Q.; Feng, J.-K.; Zhang, G.; Li, W.-K.; Cui, Y.-H.; Sun, Ch.-Ch. *Eur. J. Inorg. Chem.* **2006**, 2808.
- (26) Wang, Y.; Quillian, B.; Wei, P.; Wang, H.; Yang, X.-J.; Xie, Y.; King, R. B.; Schleyer, P. v. R.; Schaefer, H. F., III; Robinson, G. H. *J. Am. Chem. Soc.* **2005**, 127, 11944.
- (27) Zhu, Z.; Wright, R. J.; Olmstead, M. M.; Rivard, E.; Brynda, M.; Power, P. P. *Angew. Chem., Int. Ed.* **2006**, 45, 5807.

Scheme 1. Optimization of the Synthesis of Compound **1**

we also attempted the preparation of half-sandwich alkyl or aryl derivatives ($\eta^5\text{-Cp}'$) ZnR of differently substituted Cp' ligands (from now Cp' is used as a general representation for a cyclopentadienyl ligand) including C_5Me_5 . Information on these compounds is sparse, and even if some derivatives of this kind derived from the parent zincocene were known,²⁹ analogous ($\eta^5\text{-C}_5\text{Me}_5$) ZnR species had been largely overlooked, despite the fact that $\text{Zn}(\text{C}_5\text{Me}_5)_2$ (**3**) is a well-known compound, structurally characterized by X-ray crystallography and by gas electron diffraction studies.

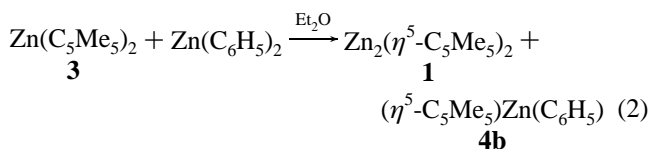
In accord with the reported formation of ($\eta^5\text{-C}_5\text{H}_5$) ZnEt as the exclusive product of the reaction of $\text{Zn}(\text{C}_5\text{H}_5)_2$ and ZnEt_2 ,^{29b} the room temperature interaction of **3** and ZnMe_2 gives ($\eta^5\text{-C}_5\text{Me}_5$) ZnMe in almost quantitative yield.^{30a} However, the use of ZnEt_2 causes the reaction to take an unexpected course, as a mixture of two compounds, the expected half-sandwich^{30a} ($\eta^5\text{-C}_5\text{Me}_5$) ZnEt (**4a**) and the unexpected dizincocene **1**, is generated (eq 1).



Low-temperature ^1H NMR monitoring and the use of different solvents permit optimization of this reaction to obtain one of the two possible compounds as the major reaction product. As represented in Scheme 1, effecting the reaction in pentane at -60°C yields exclusively the ethyl derivative **4a**, while, in Et_2O at -10°C , dizincocene **1** becomes the main reaction product, although it is always accompanied by variable amounts of **4a**. The maximum yield of **1** is seldom higher than 30% and is often significantly smaller. Indeed this reaction seems to be sensitive to subtle effects, including the purity of the reagents, and although if it has been reproduced innumerable times, on

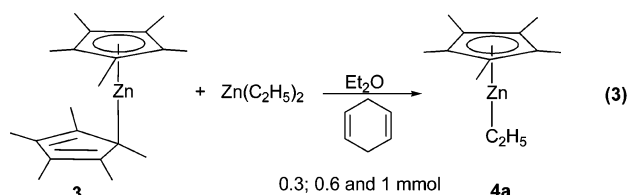
other occasions, for reasons that escape our understanding, only **4a** is formed. As discussed below, a convenient and reproducible procedure for the gram-scale synthesis of **1** has been developed.

Interestingly, while under the conditions specified above for the synthesis of **1** from **3** and ZnEt_2 , the organozinc reagents ZnPr'_2 and ZnMe_2 ($\text{Mes} = \text{C}_6\text{H}_2\text{-2,4,6-Me}_3$) furnish only the half-sandwich products ($\eta^5\text{-C}_5\text{Me}_5$) ZnR ($\text{R} = \text{Pr}'$, Me), $\text{Zn}(\text{C}_6\text{H}_5)_2$ behaves like ZnEt_2 and gives rise to almost 1:1 mixtures of $\text{Zn}_2(\eta^5\text{-C}_5\text{Me}_5)_2$ and ($\eta^5\text{-C}_5\text{Me}_5$) $\text{Zn}(\text{C}_6\text{H}_5)$ **4b** (eq 2). In practice, this method is even more limited than that of Scheme 1 due to the lower solubility in ether of the phenyl zinc organometallics involved in the reaction. The zincocenes ZnCp'_2 , when $\text{Cp}' = \text{C}_5\text{Me}_4\text{H}$, $\text{C}_5\text{Me}_4\text{SiMe}_3$, and $\text{C}_5\text{Me}_4\text{Bu}'$, react with ZnEt_2 in Et_2O to afford only the corresponding half-sandwich ethyl products, ($\eta^5\text{-Cp}'$) ZnEt .



The formation of **1** and ($\eta^5\text{-C}_5\text{Me}_5$) ZnR ($\text{R} = \text{Et}$, **4a**; C_6H_5 , **4b**) in the reaction of **3** with the corresponding ZnR_2 reagent takes place through independent, competitive reaction routes. Thus, a mixture of **1** and **4a** or **4b** remains unchanged while stirring at room temperature for 1–2 h and compounds **4** do not transform into **1** when stirred overnight at 20°C . It appears likely that the mixed compounds ($\eta^5\text{-C}_5\text{Me}_5$) ZnR form through binuclear hydrocarbyl-bridged intermediates similar to those involved in Schlenk-type equilibria, but a rationalization for the generation of **1** is more difficult. It has been suggested^{23b} that active zinc resulting from partial decomposition of ZnEt_2 may reduce **3** to **1**, but this appears unlikely as we have found that Rieke-zinc is not a sufficiently strong reductant to effect this transformation.

Instead, we have obtained evidence in favor of a radical process. In a sealed NMR tube experiment equimolar amounts of **3** and ZnEt_2 were mixed at -80°C in $(\text{C}_2\text{D}_5)_2\text{O}$ and the mixture was subsequently warmed to -10°C . Formation of **1** plus smaller amounts of **4a** was observed. Minor quantities of $\text{C}_5\text{Me}_5\text{H}$ and C_2H_6 were also detected. However, no ethylene could be detected. In view of the very high reactivity of the system toward adventitious water we have not pursued this experiment any further. Reacting **3** and ZnEt_2 in the presence of 1,4-cyclohexadiene (eq 3) gives only the half-sandwich complex **4a**, and similarly, carrying out the reaction in the presence of the free radical TEMPO (TEMPO = 2,2,6,6-tetramethylpiperidin-1-yloxy) also inhibits the formation of the dizincocene. Thus in the presence of 0.3 equiv of TEMPO, **4a**



becomes the only organometallic product, and small amounts

- (28) (a) Fernández, R.; Resa, I.; del Río, D.; Carmona, E.; Gutierrez-Puebla, E.; Monge, A. *Organometallics* **2003**, *22*, 381. (b) Resa, I.; Rodriguez, A.; Grirrane, A.; Fernandez, R.; Alvarez, E.; Carmona, E.; Gutierrez-Puebla, E.; Monge, A.; del Río, D.; Galindo, A., to be submitted.
- (29) (a) Aoyagi, T.; Shearer, H. M. M.; Wade, K.; Whitehead, G. *J. Organomet. Chem.* **1978**, *146*, C29. (b) Haaland, A.; Samdal, S.; Seip, R. *J. Organomet. Chem.* **1978**, *153*, 187. (c) Jastrzebski, J. T. B. H.; Boersma, J.; van Koten, G.; Smeets, W. J. J.; Spek, A. L. *Recl. Trav. Chim. Pays-Bas* **1988**, *107*, 263. (d) Strohmeier, W.; Ladsfeld, H. *Z. Naturforsch.* **1960**, *15b*, 332.
- (30) (a) Resa, I.; Rodriguez, A.; Alvarez, E.; Carmona, E., to be submitted. (b) Alvarez, E.; Grirrane, A.; Resa, I.; del Río, D.; Rodriguez, A.; Carmona, E. *Angew. Chem., Int. Ed.* **2006**, in press.

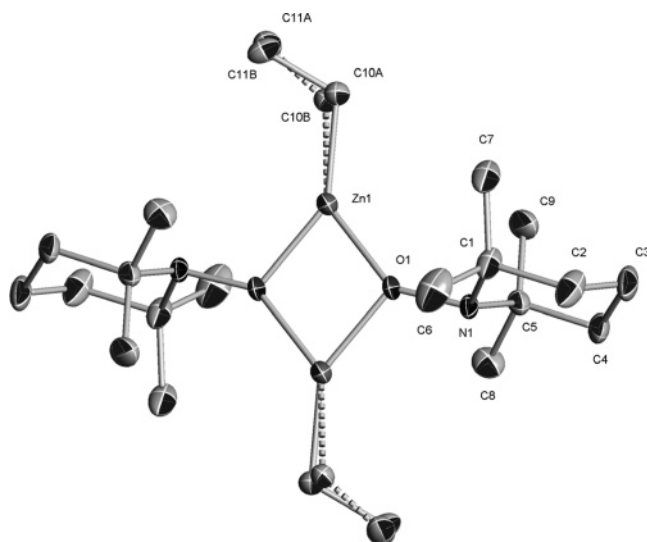
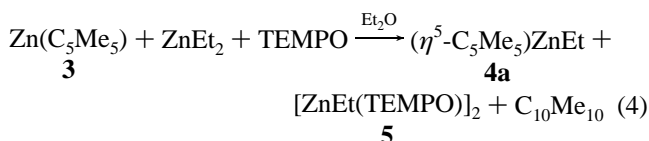


Figure 2. ORTEP representation of **5** (30% probability displacement ellipsoids).

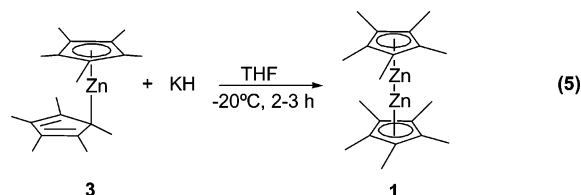
of $C_{10}Me_{10}$ resulting from the coupling of two $C_5Me_5^{\bullet}$ radicals³¹ are also detected. The use of 0.6 or 1 equiv of TEMPO increases the proportion of $C_{10}Me_{10}$ in the reaction mixture and produces also small, albeit isolable amounts of the binuclear compound **5** (eq 4) that contains a TEMPO⁻ derived bridging anionic ligand, as demonstrated by X-ray studies (Figure 2; see Supporting Information). It is important to note that the radical TEMPO does not react separately with either **3** or $ZnEt_2$, so that the above changes occur only when it is added to the mixture of the two organozinc compounds, **3** and $ZnEt_2$.



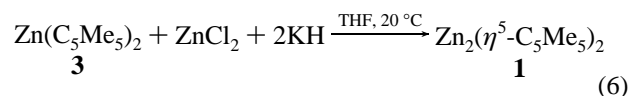
As zirconocenes $ZnCp'_2$ are good Cp' transfer reagents, it is conceivable that in ether solvents $C_5Me_5^-$ transfer from $Zn(C_5Me_5)_2$ to $ZnEt_2$ may give rise to $[Zn(C_5Me_5)_n]^+$ and $[Zn(C_5Me_5)_2Et]^-$ species. In fact, in the presence of the macrocyclic 14N4 ligands (14N4 = 1,4,8,11-tetramethyl-1,4,8,11-tetraazacyclotetradecane), $ZnEt_2$ and $ZnPh_2$ are reported to exist in equilibrium³² with $[ZnEt(14N4)]^+$ and $[ZnPh_2Et]^-$. The C_5Me_5 -containing zinc cation and anion could eventually give rise to the $Zn_2(\eta^5-C_5Me_5)_2$ product, but in the absence of additional, relevant experimental data further speculation does not seem to be justified. Nonetheless, it seems plausible that **1** may result from the coupling of $(C_5Me_5)Zn^{\bullet}$ radicals, and in this regard it should be mentioned that the formation of such radicals had already been proposed.³³ In 1985 Boersma and co-workers found that the reaction of $Zn(C_5Me_5)_2$ and $Ni(cod)_2$ yields $[(\eta^5-C_5Me_5)-Ni]_2(C_{16}H_{24})$ together with metallic zinc. The $C_{16}H_{24}$ organic ligand that bridges the two $(\eta^5-C_5Me_5)Ni$ units results from the coupling of two cyclooctadiene-derived radicals, and the zinc

metal generated in the reaction was suggested to arise from the decomposition of $(C_5Me_5)Zn^{\bullet}$ radicals.³³ Considering that solutions of **1** are exceedingly sensitive toward atmospheric reagents with formation of finely divided zinc metal, it appears probable that had $Zn_2(C_5Me_5)_2$ formed during the reaction of $Zn(C_5Me_5)_2$ and $Ni(cod)_2$ it would have decomposed under the reaction conditions (60 °C, 24 h).³³

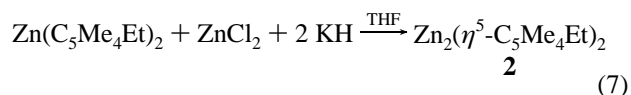
$Zn(C_5Me_5)_2$ reduction under appropriate conditions has proved to be a convenient procedure for the preparation of **1** in a ca. 2 g scale. Low-temperature reduction of **3** itself (eq 5) with a variety of reagents yields **1**. Strong reductants like Na,



K, and their hydrides, MH, as well as K/naphthalene or CaH_2 may be used, but in our hands KH is the most convenient reagent. To optimize the reduction further, mixtures of **3** and $ZnCl_2$ are reduced by KH (1:1:2 ratio) employing THF as the solvent (eq 6).



Extension of this methodology to the synthesis of dizincocenes $Zn_2Cp'_2$ of other cyclopentadienyl ligands has met so far with only limited success. Thus, zincocenes derived from C_5Me_4H , $C_5Me_4SiMe_3$, and $C_5Me_4Bu^t$ yield only zinc metal and other decomposition products under the conditions of eq 6. Interestingly, the parent zincocene, $Zn(C_5H_5)_2$, does not undergo decomposition but provides instead crystalline solids. Nevertheless the crystalline materials do not correspond to the desired dizincocene, $Zn_2(\eta^5-C_5H_5)_2$, that remains still an elusive, unknown molecule but to cyclopentadienyl zincates of composition $Zn(C_5H_5)_3^-$ and $Zn_2(C_5H_5)_5^-$ to be reported elsewhere.^{30b} Notwithstanding, $Zn(C_5Me_4Et)_2$, readily obtained from $ZnCl_2$ and KC_5Me_4Et ,^{28b} undergoes reduction under similar conditions to give $Zn_2(\eta^5-C_5Me_4Et)_2$ (**2**), the second example of a dimetalocene (eq 7).

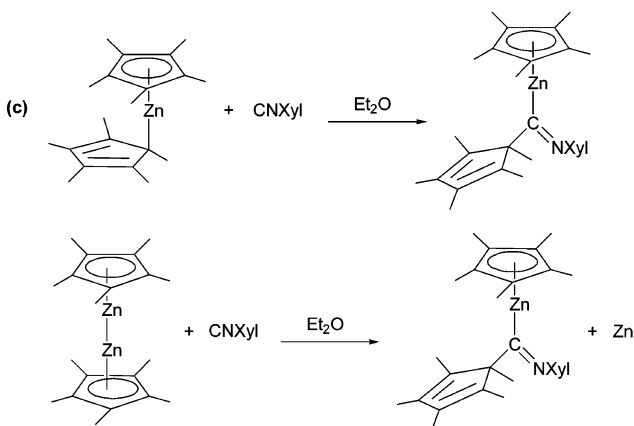
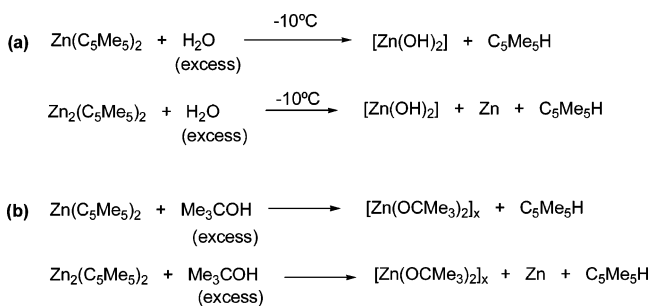


Compounds **1** and **2** can be obtained as crystalline solids. The two compounds are exceedingly reactive toward oxygen and water, but **1** has superior thermal stability and it is easier to handle than **2**. Compound **1** is a colorless crystalline solid that burns spontaneously upon exposure to air. It is indefinitely stable at room temperature under argon or in a sealed tube in vacuo and crystallizes readily from pentane or from Et_2O solutions. It decomposes at ca. 110 °C (capillary tube under argon), but it can be sublimed at temperatures near 70 °C under a dynamic vacuum of 10^{-3} mbar. The sublimed solid features 1H and $^{13}C\{^1H\}$ NMR spectra (vide infra) identical to those of samples obtained by crystallization from pentane at -20 °C. The less symmetric compound **2** is more difficult to handle than

(31) Cummins, C. C.; Schrock, R. R.; Davies, W. M. *Organometallics* **1991**, *10*, 3781.

(32) Fabicon, R. M.; Pajerski, A. D.; Richey, H. G., Jr. *J. Am. Chem. Soc.* **1991**, *113*, 6680.

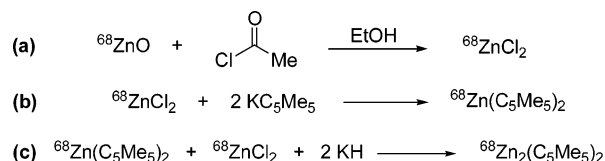
(33) (a) Fisher, B.; Boersma, J.; Kojić-Prodić, B.; Spek, A. L. *J. Chem. Soc., Chem. Commun.* **1985**, 1237. (b) Fisher, B.; Boersma, J.; van Koten, G.; Spek, A. L. *New J. Chem.* **1988**, *12*, 613

Scheme 2. Some Reactions of Metallocenes **1** and **3**

1, as it is more difficult to crystallize. In solution it exhibits moderate thermal stability at room temperature, but as a pure solid it decomposes slowly at temperatures between 0 and 20 °C and becomes a brown oily material. Heating the pure solid at 40 °C gives a deposit of metallic zinc. However, crystals of **2** suitable for X-ray studies can be obtained by slow evaporation of its pentane solutions at –20 °C or by rapidly cooling very concentrated solutions from room temperature to –78 °C, and this has allowed its structural characterization by X-ray crystallography. Because of the superior thermal stability of **1** and its easier isolation and manipulation, it has been used for the reactivity studies discussed below.

Despite the high reactivity of $\text{Zn}_2(\eta^5\text{-C}_5\text{Me}_5)_2$ toward O_2 and moisture, no reaction occurs with H_2 (1–4 atm, 20–70 °C), carbon monoxide or carbon dioxide (20 °C, 1 atm). Furthermore, compound **1** is recovered unaltered upon stirring at room temperature in the presence of NEt_3 , $\text{Me}_2\text{NCH}_2\text{CH}_2\text{NMe}_2$, pyridine or bipyridine. Similarly, no reaction takes place at 20 °C when **1** is treated with PMe_3 or PPh_3 . In all these cases some decomposition of **1** to metallic zinc is observed, but this is probably due to the action of adventitious water. Elemental iodine oxidizes **1** to a mixture of **3** and ZnI_2 (the latter identified by powder X-ray diffraction) whereas ZnMe_2 and ZnMe_2 convert **1** into mixtures of the corresponding half-sandwich compounds $(\eta^5\text{-C}_5\text{Me}_5)\text{ZnR}$, and zinc metal.

Comparison of the reactivity of the mononuclear and binuclear zirconocenes, **3** and **1**, respectively, toward H_2O , Bu^iOH , and CNXyl ($\text{Xyl} = \text{C}_6\text{H}_3\text{-2,6-Me}_2$) is useful (Scheme 2). The mononuclear zirconocene reacts with water at –10 °C (a 10 molar excess, dilute Et_2O solution) forming $\text{C}_5\text{Me}_5\text{H}$ and a white precipitate of $\text{Zn}(\text{OH})_2$ that gives into ZnO when heated at 50 °C under a vacuum. The analogous reaction of **1** generates $\text{C}_5\text{-Me}_5\text{H}$, $\text{Zn}(\text{OH})_2$, and highly crystalline zinc metal, as shown by X-ray powder diffraction, but upon workup at 20 °C, H_2

Scheme 3. Synthesis of $^{68}\text{Zn}_2(\eta^5\text{-C}_5\text{Me}_5)_2$ 

evolution is clearly observed (confirmed by ^1H NMR experiments) as a result of reduction of H_2O by the reactive zinc produced. After heating the solid at 50 °C under a vacuum, ZnO is obtained as the only metal-containing product. The alcoholysis of the zirconocenes by Bu^iOH yields related results. Thus **3** affords $\text{C}_5\text{Me}_5\text{H}$ and $[\text{Zn}(\text{OBu}^i)_2]_x$ (Scheme 2b), whereas the zinc–zinc bonded metallocene yields a mixture of $\text{C}_5\text{Me}_5\text{H}$, Zn , and $[\text{Zn}(\text{OBu}^i)_2]_x$. Metallic zinc and the alkoxide have been identified by X-ray powder diffraction, and the latter has been identified also by comparison of its ^1H and $^{13}\text{C}\{^1\text{H}\}$ NMR spectra with those of an authentic sample.³⁴

Finally, CNXyl reacts with compound **3** to give the iminoacyl product **6** (Scheme 2c), also identified by comparison of its spectroscopic properties (IR, ^1H and $^{13}\text{C}\{^1\text{H}\}$ NMR) with those of an authentic sample.³⁵ The analogous reaction of **1** yields the iminoacyl **6** plus metallic zinc, as the only reaction products. Thus, it is clear that, under the conditions specified in Scheme 2, H_2O , Bu^iOH , and CNXyl induce the disproportionation of **1** into Zn and the corresponding $\text{Zn}(\text{II})$ compound.

Molecular Structures of $\text{Zn}_2(\eta^5\text{-C}_5\text{Me}_5)_2$ and $\text{Zn}_2(\eta^5\text{-C}_5\text{Me}_4\text{Et})_2$. Compound **1** has been structurally characterized by several independent methods, including NMR, mass spectrometry, vibrational spectroscopy (IR and Raman studies, to be reported elsewhere³⁶), and X-ray diffraction studies. A neutron diffraction investigation on compound **1** has also been carried out independently and will be reported separately.³⁷ Since a cobalt complex initially formulated as $\text{Co}_2(\eta^5\text{-C}_5\text{Me}_5)_2$ ^{10a} was subsequently demonstrated to contain three bridging hydrogen atoms, $[(\eta^5\text{-C}_5\text{Me}_5)\text{Co}]_2(\mu\text{-H})_3$,^{10b–d} we have applied the above techniques to discard a putative bridging hydride structure for our compounds, i.e., $[(\eta^5\text{-Cp}^i)\text{Zn}]_2(\mu\text{-H})_2$. Further verification of the composition of **1** was provided by mass spectral analysis of $^{68}\text{Zn}_2(\eta^5\text{-C}_5\text{Me}_5)_2$, which was prepared from commercially available ^{68}ZnO via Scheme 3.

None of the above techniques have given any indication for the existence of zinc-bound hydrogen atoms, $\text{Zn}(\mu\text{-H})_2\text{Zn}$. Instead their application support the dimetalocene formulation, with a direct $\text{Zn}\text{--}\text{Zn}$ bond. Because of the poor thermal stability of compound **2** its characterization relies on solution ^1H and $^{13}\text{C}\{^1\text{H}\}$ NMR data and on a low-temperature X-ray diffraction study. As discussed below, comparison of the $\text{Zn}\text{--}\text{Zn}$ distance in **1** and **2** (ca. 2.31 Å) with those found in known $\text{Zn}_2(\mu\text{-H})_2$ compounds^{27,38} (ca. 2.45 Å), corroborate the proposed formulation. Theoretical calculations presented in the next section and those already in the literature^{22b,24,25} give additional strength to the proposal that **1** and **2** have unique dimetalocene structures.

(34) Coates, G. E.; Roberts, P. D. *J. Chem. Soc. A* **1967**, 1233.

(35) Lopez del Amo, J. M.; Buntkowsky, G.; Limbach, H. -H.; Resa, I.; Fernandez, R.; Carmona, E., submitted.

(36) Tang, C.; Downs, A. J.; Koeppe, R.; Resa, I.; Rodriguez, A.; Carmona, E., manuscript in preparation.

(37) Fernández-Díaz, M. T.; McIntyre, G.; Gutiérrez-Puebla, E.; Monge, A., manuscript in preparation.

(38) Hao, H.; Cui, C.; Roesky, H. W.; Bay, G.; Schmidt, H. -G.; Moltemeyer, M. *Chem. Commun.* **2001**, 1118.

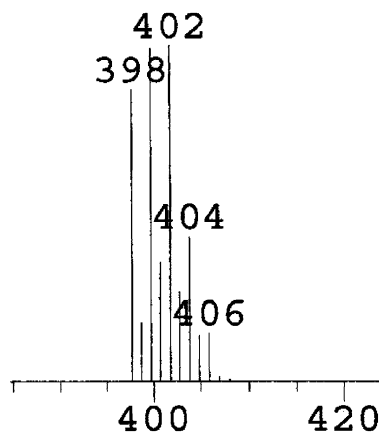


Figure 3. Molecular ion envelope M^+ for **1**.

The ^1H and $^{13}\text{C}\{^1\text{H}\}$ NMR spectra of **1** are extremely simple and of little structural value. The ^1H NMR spectrum shows only one signal at δ 2.02 due to the Me protons of the C_5Me_5 ligands. A corresponding $^{13}\text{C}\{^1\text{H}\}$ resonance is found at δ 10.0, and this is accompanied by the resonance due to the quaternary ring carbon nuclei with a chemical shift of 108.8 ppm. No ^1H signals attributable to a putative bis(hydride) bridging structure have been found. For comparative purposes, the structurally characterized bridging hydride complexes $[\text{HC}(\text{CMeNXyl})_2]\text{Zn}_2(\mu\text{-H})_2$ ³⁸ and $[\text{ArZn}]_2(\mu\text{-H})_2$ ²⁷ (Ar = $\text{C}_6\text{H}_3\text{-}2,6\text{-}(\text{C}_6\text{H}_3\text{-}2,6\text{-Pr}'_2)_2$) present signals at 4.59 and 4.84 ppm, respectively, due to the hydride ligands. NMR data for **2** are also simple, and as for **1** they are of little use for structural purposes. These data are listed in the Experimental Section.

The high-resolution mass spectra of **1** and the ^{68}Zn -labeled compound provide unequivocal support for the dimetalloocene formulation, $\text{Zn}_2(\eta^5\text{-C}_5\text{Me}_5)_2$, without additional H atoms. Figure 3 shows the molecular ion envelope, M^+ around 400 m/e, whose complexity is due to the existence of several zinc isotopes (principally ^{64}Zn , 48.6%; ^{66}Zn , 27.9%; ^{67}Zn , 4.1%; and ^{68}Zn , 18.8%³⁹). It is evident that the dimeric molecules of **1** give a well behaved molecular ion in the gas phase. The exact mass of the peak at 398 amu is 398.0927, giving an excellent fit for the calculated mass of 398.0930 for $^{64}\text{Zn}_2^{12}\text{C}_{20}^1\text{H}_{30}$, whereas the exact mass of the peak at 400 amu (400.0904) corresponds to the molecules with isotopic distribution $^{64}\text{Zn}^{66}\text{Zn}^{12}\text{C}_{20}^1\text{H}_{30}$. The artificially prepared $^{68}\text{Zn}_2(\text{C}_5\text{Me}_5)_2$ gives a simple molecular ion M^+ at 406 amu, exact mass 406.0848, due to molecules with isotopic distribution $^{68}\text{Zn}_2^{12}\text{C}_{20}^1\text{H}_{30}$ (calculated mass 406.0844). In the two spectra, fragment ion patterns due to $\text{Zn}(\text{C}_5\text{Me}_5)_2$ and $^{68}\text{Zn}(\text{C}_5\text{Me}_5)_2$ are respectively observed, suggesting that in the gas phase the molecules of $\text{Zn}_2(\text{C}_5\text{Me}_5)_2$ rearrange to $\text{Zn}(\text{C}_5\text{Me}_5)_2$ and Zn.

The crystal and molecular structures of the dimetalloenes **1** and **2** have been determined by X-ray crystallography and are presented in Figures 4 and 5 (see Experimental Section for X-ray data). For **1** two independent determinations have been carried out, the first at -100 °C using graphite monochromated Mo K_α radiation ($\lambda = 0.71073$ Å), while the second was effected at -170 °C, with Cu K_α radiation ($\lambda = 1.54184$ Å). In accord with expectations both determinations provided identical results, and hence only the original -100 °C study is discussed. As can be seen in Figure 4, the zinc atoms are sandwiched between

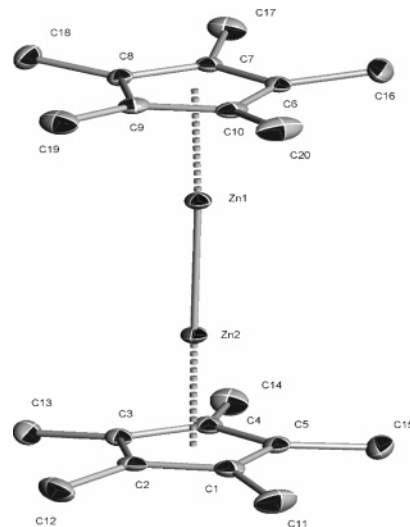


Figure 4. ORTEP representation for **1** (30% probability displacement ellipsoids). $d(\text{Zn}-\text{Zn}) = 2.305(3)$ Å. $\text{C}_5\text{Me}_5\text{centr}-\text{Zn}-\text{Zn}$ angles $177.05(2)^\circ$ and $178.88(2)^\circ$.

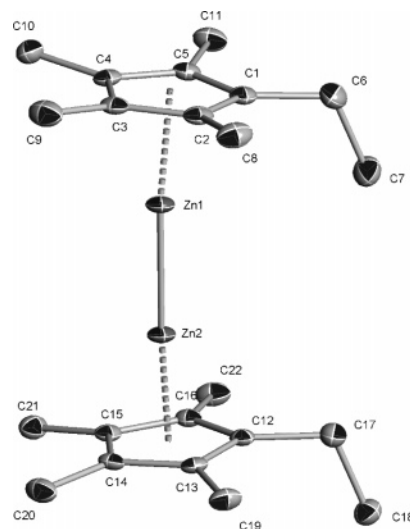


Figure 5. ORTEP representation for **2** (30% probability displacement ellipsoids). $d(\text{Zn}-\text{Zn}) = 2.295(3)$ Å. $\text{C}_5\text{Me}_4\text{Etcentr}-\text{Zn}-\text{Zn}$ angles $173.60(1)^\circ$ and $176.77(2)^\circ$.

two planar, nearly parallel C_5Me_5 rings that adopt an eclipsed configuration. The separation between the planes of the rings is of ca. 6.40 Å, and as the van der Waals radius assigned to a $-\text{CH}_3$ group is of 2.0 Å,⁴⁰ this large distance prevents steric interactions between Me groups of the two rings that are common in mononuclear metallocenes.⁴¹ This notwithstanding, the Me groups bent out of the plane of the rings away from the metal atoms, the ring plane-C-Me angles varying between ca. 3° and 6° . Similar bendings have been observed in mononuclear metallocenes and have been attributed, using covalency arguments,⁴² to the match between the radial extensions of the p-orbitals of the metal parallel to the Cp' ring and the carbon p-orbitals of the Cp' ring perpendicular to the Cp' plane. Alternatively, on an electrostatic description as applied

(39) Emsley, J. *The Elements*, 2nd ed.; Clarendon Press: Oxford, 1991.

(40) Pauling, L. *The Nature of the Chemical Bond*, 3rd ed.; Cornell University Press: Ithaca, New York, 1960; Chapter 7.

(41) (a) Haaland, A. *Acc. Chem. Res.* **1979**, *12*, 415. (b) Haaland, A. *Top. Curr. Chem.* **1975**, *53*, 1.

(42) Jemmis, E. D.; Schleyer, P. v. R. *J. Am. Chem. Soc.* **1982**, *104*, 4781.

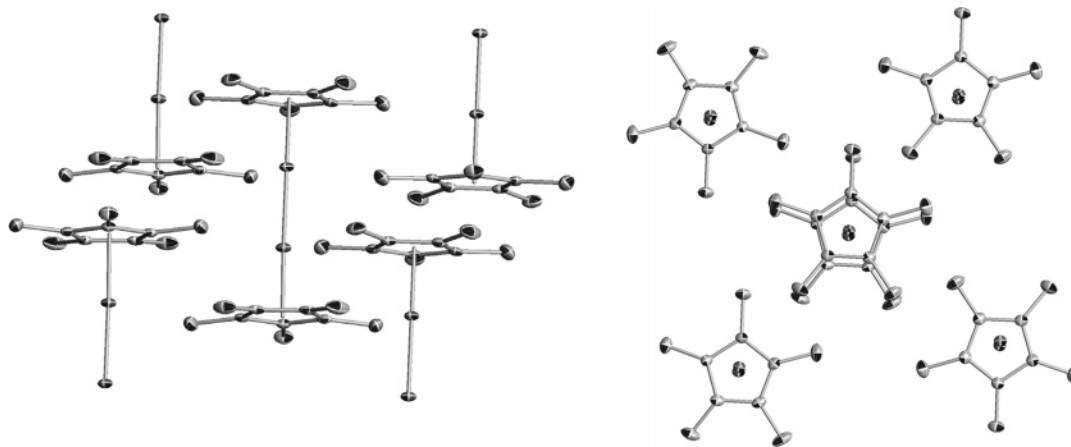


Figure 6. Crystal packing of compound **1** showing one $\text{Zn}_2(\eta^5\text{-C}_5\text{Me}_5)_2$ molecule and the specific orientation of four neighbor molecules (for which only one C_5Me_5 ring is shown).

to LiC_5H_5 ,⁴³ it has been advanced that a positively charged metal center will favor greater electron density on its side of the Cp' ring, achieved by bending the ring substituents away from the metal.⁴³

In compound **1** the coordination of the C_5Me_5 rings is symmetrical and it is characterized by $\text{Zn}-\text{C}_{\text{ring}}$ distances in the narrow range of 2.27 to 2.30 Å and by $\text{Zn}-\text{C}_5\text{Me}_5_{\text{centr}}$ separations of ca. 2.04 Å. Furthermore, the $\text{ring}_{\text{centr}}-\text{Zn}-\text{Zn}-\text{ring}_{\text{centr}}$ distribution is almost linear, with an average angle of $177.4(1)^\circ$. The molecular structure of $\text{Zn}_2(\eta^5\text{-C}_5\text{Me}_4\text{Et})_2$ exhibits similar features (Figure 5) although the $\text{ring}_{\text{centr}}-\text{Zn}-\text{Zn}-\text{ring}_{\text{centr}}$ shows some deviation from linearity, with $\text{ring}_{\text{centr}}-\text{Zn}-\text{Zn}$ angles of $173.6(1)^\circ$ and $176.8(1)^\circ$.

Doubtless, the most salient feature in the structures of **1** and **2** is the short $\text{Zn}-\text{Zn}$ separation of 2.305(3) Å in **1** and 2.295(2) Å in **2**, thus identical within experimental error. For the two compounds, the $\text{Zn}-\text{Zn}$ bond length is appreciably shorter than twice Pauling's single-bond metallic radius (2.50 Å⁴⁰). Comparing this $\text{Zn}-\text{Zn}$ distance with the $\text{M}-\text{M}$ bond lengths in $\text{Cd}_2(\text{AlCl}_4)_2$ ³ and the dimercury dihalides Hg_2X_2 ^{12,44} is noteworthy. In the Cd_2 compound the $\text{Cd}-\text{Cd}$ distance is 2.58 Å, while twice Pauling's single bond metallic radius for the Cd atom is 2.82 Å. The reduction of ca. 8% is comparable to that corresponding to the Zn_2 compounds **1** and **2**, while, for mercury, taking the $\text{Hg}-\text{Hg}$ separation of 2.53 Å corresponding to Hg_2Cl_2 and the metallic radius of 1.44 Å, the reduction is of about 12%. Comparison with the $\text{Zn}-\text{Zn}$ separation in the other two zinc–zinc bonded compounds known and in reported $\text{Zn}(\mu\text{-H})_2\text{Zn}$ structures is also appropriate. Thus, in Robinson's $\text{Zn}_2[\text{HC}(\text{CMeNAr})_2]_2$ ²⁶ and Power's²⁷ $\text{Zn}_2\text{Ar}'_2$ (vide supra for the meaning of Ar and Ar'), the $\text{Zn}-\text{Zn}$ bond distances are essentially the same, ca. 2.36 Å, that is, about 0.05 Å longer than in **1** and **2**, despite the lower effective coordination number of the metals, in comparison with **1** and **2**. In the H-bridged dimers $[\text{HC}(\text{CMeNAr})_2]_2\text{Zn}_2(\mu\text{-H})_2$ ³⁸ and $[\text{Ar}'\text{Zn}]_2(\mu\text{-H})_2$ ²⁷ where there is no zinc–zinc bond, the metal–metal distances are 2.45 and 2.41 Å, respectively, between 0.1 and 0.15 Å longer than in the $\text{Zn}_2(\eta^5\text{-Cp}')_2$ compounds **1** and **2**. Additionally, it is worth noting that in the compounds $\text{Ar}'\text{ZnZnAr}'$ and $[\text{Ar}'\text{Zn}]_2(\mu\text{-H})_2$, where the aryl ligands remain the same,²⁷ the $\text{Zn}-\text{Zn}$ distances of 2.3591(9) Å and 2.4084(3) Å differ by only ca. 0.05 Å.

Interestingly, the related $[\text{Ar}'\text{Zn}]_2(\mu\text{-H})(\mu\text{-Na})$ derivative that exhibits an unusual type of metal–metal interaction has a $\text{Zn}-\text{Zn}$ separation of 2.352(2) Å, thus essentially identical to that of $\text{Ar}'\text{ZnZnAr}'$.²⁷

A final structural comment that is worthy of note concerns the molecular packing observed in the crystals of **1** and **2**. With reference for instance to **1** (see Figure 6) each molecule of $\text{Zn}_2(\eta^5\text{-C}_5\text{Me}_5)_2$ is surrounded by four neighbor molecules with an orientation such that all of the $\text{Zn}-\text{Zn}$ vectors are parallel and consequently the C_5Me_5 rings are also parallel. If these molecules are viewed along the $\text{Zn}-\text{Zn}$ vector of one molecule of $\text{Zn}_2(\eta^5\text{-C}_5\text{Me}_5)_2$, the cyclopentadienyl ligands are found to adopt a gearlike arrangement with each C_5Me_5 group being located approximately at the midpoint of the $\text{Zn}-\text{Zn}$ vector and perpendicular to it.

Electronic Structure and Bonding Properties of **1 and **2**. Comparison with Other $\text{Zn}-\text{Zn}$ Bonded Species.** The synthesis and structural characterization of **1** was followed shortly by a number of theoretical studies aimed at investigating the electronic structure and the bonding characteristics of $\text{Zn}_2(\eta^5\text{-C}_5\text{Me}_5)_2$ and of other related species. Here we provide full details^{22b} of our own computational analysis of $\text{Zn}_2(\eta^5\text{-C}_5\text{Me}_5)_2$ extended to other dizincocenes $\text{Zn}_2(\eta^5\text{-Cp}')_2$ and to compounds of general formulation Zn_2R_2 . The stability of these molecules has been calculated with the aid of DFT methods by computing their $\text{Zn}-\text{Zn}$ bond dissociation energy and the energy of their disproportionation reaction to metallic zinc and the corresponding $\text{Zn}(\text{II})$ organometallic, ZnCp'_2 or ZnR_2 .

One of our initial targets was the investigation of the unusual $\text{Zn}-\text{Zn}$ bond. The interaction of a Cp' ligand with a p block metal in monomeric $\text{Cp}'\text{M}$ species ($\text{M} = \text{In}, \text{Tl}, \text{Sn}^+$) was analyzed by Canadell and Eisenstein.⁴⁵ Recently, the CpZn unit has been studied in the parent zincoocene,^{21f} for which several coordination modes have been investigated⁴⁶ and a number of quantitative parameters computed.⁴⁷ Previous to the discussion of the DFT results and taking into account the classical MO diagram of a half-sandwich main group metallocene,^{45,48} the

(45) Canadell, E.; Eisenstein, O. *Organometallics* **1984**, *3*, 759.

(46) Lokshin, B. V.; Garkusha, O. G.; Borisov, Y. A.; Borisova, N. E. *Russ. Chem. Bull. Int. Ed.* **2003**, *52*, 831.

(47) Rayón, V. M.; Frenking, G. *Chem.—Eur. J.* **2002**, *8*, 4693.

(48) For example, see: Kwon, C.; McKee, M. L. In *Computational Organometallic Chemistry*; Cundari, T. R., Ed.; Marcel Dekker: New York, 2001; p 397.

(43) Waterman, K. C.; Streitwieser, A., Jr. *J. Am. Chem. Soc.* **1984**, *106*, 3138.

(44) Dorn, E. *J. Chem. Soc., Chem. Commun.* **1971**, 466.

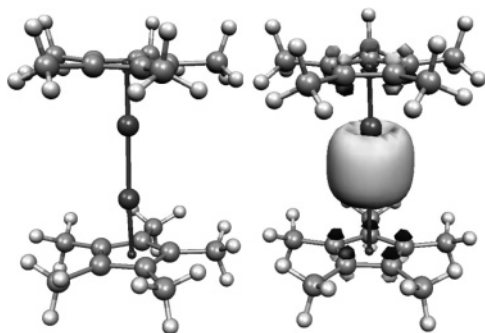


Figure 7. Optimized structure of $\text{Zn}_2(\eta^5\text{-C}_5\text{Me}_5)_2$ compound and 3D-isosurface of the HOMO-4, which corresponds to the Zn–Zn interaction.

frontier orbitals of a neutral $(\eta^5\text{-C}_5\text{Me}_5)\text{Zn}$ group are a singly occupied HOMO, which results from the antibonding combination of a_1 (π , Cp^*) and the s and p_z metal orbitals and a pair of degenerate orbitals that are the combination of e_1 (π , Cp^*) with the $p_{x,y}$ metal orbitals. Thus, from a qualitative point of view, the Zn–Zn bond in **1** results from the interaction of the singly occupied HOMOs of the two $(\eta^5\text{-C}_5\text{Me}_5)\text{Zn}$ fragments. These qualitative arguments are fully confirmed by our DFT calculations.²² The MO distribution of $\text{Zn}_2(\eta^5\text{-C}_5\text{Me}_5)_2$ was analyzed by using the AOMIX program,^{49,50} to find four quasi-degenerate occupied orbitals (from the HOMO to the HOMO-3) that are the combinations (in-phase and out-of-phase) of the degenerate e_1 orbitals of C_5Me_5 with a very small participation of the p orbitals of Zn atoms (less than 3%). The HOMO-4 (Figure 7) corresponds to the Zn–Zn interaction and has a participation of Zn orbitals close to 60% (s , 96%, and p , 4%, for each Zn atom). A similar interpretation of the bonding has been provided by Kress.^{25d} In the β -diketiminato complex $\text{Zn}_2[\text{HC}(\text{CMeNAr})_2]_2$ the Zn–Zn bond also has very high s character,²⁶ whereas the metal–metal interaction of the aryl derivative $\text{Ar}'\text{ZnZnAr}'$ results mostly from overlap of the zinc $4p_z$ orbitals.²⁷

The bond distances and angles computed for $\text{Zn}_2(\eta^5\text{-C}_5\text{Me}_5)_2$ (Figure 7) compare favorably with the experimental values (Table 1). For instance, the calculated Zn–Zn bond distance of 2.33 Å is nearly identical to the experimental value of ca. 2.30 Å found for **1** and **2**. Moreover, the calculated Zn–Zn length agrees well with values computed for a number of Zn(I) species containing the $[\text{Zn}–\text{Zn}]^{2+}$ unit. For instance, the model $\text{Zn}_2[\{\text{HNCH}_2\text{CH}\}_2]$ and the dihalides Zn_2X_2 ($\text{X} = \text{F}, \text{Cl}, \text{Br}, \text{I}$) have been computed at various levels of theory with Zn–Zn bond lengths in the range 2.28–2.39 Å.^{51,52} In addition, in the dihydride Zn_2H_2 the Zn–Zn separation is of the order of 2.37–2.40 Å.^{17a,52} Table 1 summarizes the Zn–Zn distances obtained up to now from both experimental and theoretical studies. As can be seen, except for the neutral Zn_2 and the singly charged Zn_2^\pm , these distances fall in the range 2.28–2.40 Å and are significantly lower than the 2.60 Å value computed for the $[\text{Zn}–\text{Zn}]^+$ cation.⁵³

In our preliminary report^{22b} we determined the dissociation energy of the zinc–zinc bond (BDE) by adopting a fragment-oriented approach⁵⁴ and obtained a value of 62.1 kcal·mol^{−1} for $\text{Zn}_2(\eta^5\text{-C}_5\text{Me}_5)_2$ and a similar value (62.5 kcal/mol) for Zn_2

($\eta^5\text{-C}_5\text{H}_5$)₂. The computed electronic energy $E(\text{Zn}–\text{Zn})$ (see Table 2) of about 66 kcal·mol^{−1} is comparable to values between 67 and 72 kcal·mol^{−1} reported by others for the same compound^{25b–d} and to those calculated for the dihalides Zn_2X_2 ($\text{X} = \text{F}, \text{Cl}, \text{Br}, \text{I}$)^{51,52} and Zn_2H_2 .^{17a,52} Evidently the 62 kcal·mol^{−1} value corresponding to the Zn–Zn BDE in $\text{Zn}_2(\eta^5\text{-C}_5\text{Me}_5)_2$ is higher by ca. 40 kcal·mol^{−1} than that obtained for the cationic $[\text{Zn}–\text{Zn}]^+$ species⁵³ that has a lower Zn–Zn bond order, and it is also significantly higher than the experimental value of ca. 13 kcal·mol^{−1} determined for the cation $[\text{Zn}–\text{Zn}]^+$ in a gas phase study.⁵⁵

Since the energy of the disproportionation reaction to Zn(0) and Zn(II) is a better measure of the stability of the dizinc compounds than the energy of the Zn–Zn bond,^{23b,24a} the energy of the disproportionation reaction $\text{Zn}_2\text{Cp}'_2 \rightarrow \text{Zn} + \text{ZnCp}'_2$ has been computed, assuming that gaseous zinc is produced. For the parent $\text{Zn}_2(\eta^5\text{-C}_5\text{H}_5)_2$ the reaction is endothermic by 20.0 kcal·mol^{−1}, in accord with the value obtained by Schaeffer et al.^{24a} We have computed an endergonic value of ca. 5 kcal·mol^{−1} for ΔG , this result being consistent with the stability of the compounds $\text{Zn}_2(\eta^5\text{-C}_5\text{Me}_5)_2$ and $\text{Zn}_2(\eta^5\text{-C}_5\text{Me}_4\text{Et})_2$.

In order to gain further knowledge of the dizinc unit in organometallic compounds, we have extended our theoretical study to other Zn_2R_2 molecules ($\text{R} = \text{CH}_3, \text{CF}_3, \text{SiH}_3, \text{Ph}, \text{CCH}$). The related mononuclear ZnR_2 compounds had already been investigated both experimentally and theoretically.⁵⁶ Optimized structures for these compounds are presented in Figure 8, while their structural parameters are included as Supporting Information. The energies of the Zn–Zn bond and those of the disproportionation reactions computed for these compounds are collected in Table 2. It is clear that the BDEs of between 48 and 66 kcal·mol^{−1} found for these simple organometallic molecules are similar to the corresponding values in the dimetallocenes $\text{Zn}_2(\eta^5\text{-Cp}')_2$.

Analysis of the bonding and of the MO distribution has also been performed, using the AOMIX program^{49,50} (corresponding figures for selected MOs are included in the Supporting Information). For Zn_2Me_2 and $\text{Zn}_2(\text{CF}_3)_2$ the main component of the Zn–Zn bond resides in the HOMO-2 that consists mostly (86–90%) of the Zn orbitals (about 95% s character and 3–4% d character). A similar conclusion is obtained for $\text{Zn}_2(\text{SiH}_3)_2$ and also for Zn_2Ph_2 , for which related calculations have been published recently²⁷ with similar results.

The BDEs calculated for Zn_2R_2 molecules suggest that they have sufficient stability for them to be isolated, but the energies of the disproportionation reactions indicate otherwise. Thus, thermodynamic parameters in Table 2 point to exergonic disproportionation with electron-withdrawing groups, e.g., CF_3 vs Me, providing some stabilization. The synthesis of the aryl derivative $\text{Zn}_2\text{Ar}'_2$ ²⁷ contrasts with a disproportionation energy of ca. −10 kcal·mol^{−1} computed for Zn_2Ph_2 , although it can reasonably be expected that the bulky *o*-substituents ($\text{Ar}' = \text{C}_6\text{H}_3\text{-2,6-(C}_6\text{H}_3\text{-2,6-Pr}^i_2)$) play an important stabilizing role. In any case, these theoretical predictions should be taken with caution, as significantly different values have, for example, been

(49) Gorelsky, S. I. AOMix program, rev. 5.62. <http://www.obbligato.com/software/aomix>

(50) Gorelsky, S. I.; Lever, A. B. P. *J. Organomet. Chem.* **2001**, 635, 187.

(51) Liao, M.-S.; Zhang, Q.-E.; Schwarz, W. H. E. *Inorg. Chem.* **1995**, 34, 5597.

(52) Kaupp, M.; von Schnering, H. G. *Inorg. Chem.* **1994**, 33, 4179.

(53) Gutsev, G. L.; Bauschlicher, C. W., Jr. *J. Phys. Chem. A* **2003**, 107, 4755.

(54) Rosa, A.; Ehlers, A. W.; Baerends, E. J.; Snijders, J. G.; te Velde, G. *J. Phys. Chem.* **1996**, 100, 5690.

(55) Buckner, S. W.; Gord, J. R.; Freiser, B. S. *J. Chem. Phys.* **1988**, 88, 3678.

(56) Haaland, A.; Green, J. C.; McGrady, G. S.; Downs, A. J.; Gullo, E.; Lyall, M. J.; Timberlake, J.; Tutukin, A. V.; Volden, H. V.; Østby, K.-A. *J. Chem. Soc., Dalton Trans.* **2003**, 4356.

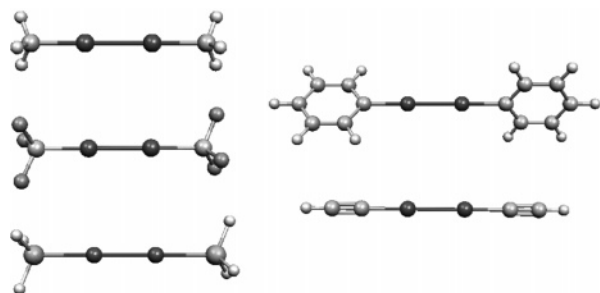
Table 1. Review of the Experimental and Calculated Zn–Zn Lengths

| compound | Zn–Zn length (Å) | comments | reference |
|--|------------------|---|-----------|
| Experimental | | | |
| Zn ₂ (η ⁵ -C ₅ Me ₅) ₂ | 2.305(3) | X-ray | this work |
| Zn ₂ (η ⁵ -C ₅ Me ₄ Et) ₂ | 2.295(3) | X-ray | this work |
| Zn ₂ {[(2,6- <i>i</i> -Pr ₂ C ₆ H ₃) N(Me)C] ₂ CH ₂ } | 2.3586(7) | X-ray | 26 |
| Zn ₂ {C ₆ H ₃ -2,6-(C ₆ H ₃ -2,6-Pr ₂) ₂ } | 2.3591(9) | X-ray | 2 |
| Theory | | | |
| Zn ₂ (η ⁵ -C ₅ Me ₅) ₂ | 2.331 | no symmetry, B3LYP | this work |
| | 2.310 | D _{5h} , B3LYP | 25b |
| | 2.287 | D _{5h} , MP2 | 25b |
| | 2.336 | D _{5h} , B3LYP | 25d |
| | 2.339 | no symmetry, B3LYP | 24d |
| Zn ₂ (η ⁵ -C ₅ H ₅) ₂ | 2.328 | no symmetry, B3LYP | this work |
| | 2.336 | D _{5h} , B3LYP | 24a |
| | 2.315 | D _{5h} , B3LYP | 24a |
| | 2.307 | D _{5h} , B3LYP | 25b |
| | 2.29 | VASP, D _{5h} | 25c |
| | 2.338 | D _{5h} , B3LYP | 24d |
| | 2.338 | D _{5h} , B3LYP | 24d |
| Zn ₂ {[HNCH] ₂ CH ₂ } | 2.392 | D _{2d} , B3LYP | 26 |
| Zn ₂ X ₂ (X = F, Cl, Br, I) | range 2.28–2.36 | several compounds, D _{∞h} | 51,52 |
| Zn ₂ H ₂ | range 2.37–2.40 | D _{∞h} | 17a,52 |
| Zn ₂ | range 3.18–3.91 | D _{∞h} , several exchange-correlation potentials | 53 |
| Zn ₂ ⁺ | 2.60 | | |
| Zn ₂ ⁻ | range 3.02–3.20 | | |
| Zn ₂ (η ⁵ -P ₅) ₂ | 2.487 | D ₅ , B3LYP | 25f |
| Zn ₂ Cp(η ⁵ -P ₅) | 2.476 | C ₅ , B3LYP | 25f |

Table 2. Calculated Energies (kcal/mol) of Zn₂R₂ Compounds for the Zn–Zn Bond Dissociation Energy (BDE), with the Computed Energy Contributions, and for the Disproportionation Reaction

| molecule | Zn–Zn bond dissociation energy | | | | disproportionation energy | | | |
|---|--------------------------------|------|------|------------------|---------------------------|----------|-------|-------|
| | E(Zn–Zn) ^a | 2-ER | BSSE | BDE ^b | ΔE | ΔE + ZPE | ΔH | ΔG |
| Zn ₂ (η ⁵ -C ₅ H ₅) ₂ | 66.7 | -2.6 | -0.8 | 62.5 | +17.5 | +17.9 | +20.0 | +4.7 |
| Zn ₂ (CH ₃) ₂ | 55.2 | -1.4 | -0.5 | 53.3 | -1.3 | -1.3 | -1.2 | -8.2 |
| Zn ₂ (CF ₃) ₂ | 59.3 | -4.8 | -0.8 | 53.7 | +3.8 | +3.7 | +3.7 | -2.9 |
| Zn ₂ (SiH ₃) ₂ | 50.2 | -1.4 | -0.4 | 48.4 | -0.2 | -0.3 | -0.3 | -5.4 |
| Zn ₂ Ph ₂ | 58.4 | -0.7 | -0.6 | 55.1 | -1.1 | -3.2 | -2.8 | -10.1 |
| Zn ₂ (CCH) ₂ | 66.6 | -0.3 | -0.7 | 65.6 | +2.2 | +2.1 | +2.1 | -4.7 |

^a The computed BDE represents only the electronic contribution to the reaction enthalpies and does not include ZPE corrections (details in the Supporting Information). ^b Corrected for BSSE.

**Figure 8.** Optimized structures of Zn₂R₂ compounds (R = CH₃, CF₃, SiH₃, Ph, CCH).

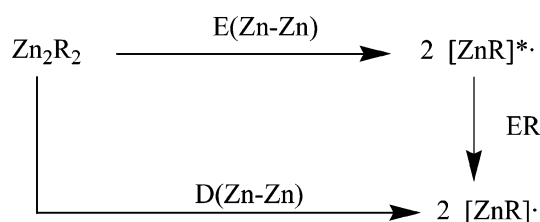
obtained^{25b} for the Zn–Zn BDE in **1** using CCSD(T) methods (ca. 42 kcal·mol⁻¹) and B3LYP calculations (ca. 67 kcal·mol⁻¹).

In summary, the original discovery of decamethyldizincocene (**1**) has been complemented with the synthesis and X-ray structural analysis of Zn₂(η⁵-C₅Me₄Et)₂ (**2**). Although the latter compound exhibits lower thermal stability than **1**, its formation suggests that analogous dizincocenes derived from differently substituted cyclopentadienyl ligands may be isolated. The two

dizincocenes can be prepared readily in ca. 1–2 g scale. Several independent structural characterization techniques prove unequivocally that they contain two directly bonded (η⁵-Cp')Zn units, with a short Zn–Zn separation of ca. 2.30 Å. Prior to the synthesis of **1**, stable, molecular compounds of the Zn₂²⁺ unit had not been reported. But, in addition, the structures of **1** and **2** are unique, as the almost linear Cp'_{centr}–Zn–Zn–Cp'_{centr} geometry, with a homonuclear metal–metal bond unsupported by bridging ligands, finds no precedent among metallocenes of either the transition series or the main group elements. The results of our DFT analysis of the electronic structure of **1** reveal that the Zn–Zn bond is strong (ca. 62 kcal·mol⁻¹), and it is formed mainly by interaction of the 4s orbitals.

Experimental Section

General Methods. All preparations and manipulations were carried out under oxygen-free argon using conventional Schlenk and glovebox techniques. Solvents were rigorously dried and degassed before use. Microanalyses were obtained at the Microanalytical Service of the Instituto de Investigaciones Químicas (Sevilla). Mass spectra were obtained at the Mass Spectroscopy Facility in the Chemistry Department

Scheme 4. Two Different Routes for Calculation of BDE

at the University of California, Berkeley. Infrared spectra were recorded on a Bruker Vector 22 spectrometer. NMR spectra were recorded on Bruker AMX-300, DRX-400, and DRX-500 spectrometers. The ^1H and ^{13}C resonances of the solvent were used as the internal standard, and the chemical shifts are reported relative to TMS.

Synthesis of $^{68}\text{ZnCl}_2$. A commercial sample of ^{68}ZnO (0.617 g, 7.31 mmol; $\geq 99\%$ enrichment) was dissolved in 22 mL of ethanol, and acetyl chloride (2.10 mL, 29.34 mmol) was added dropwise with a syringe while keeping the temperature at 0°C . The mixture was allowed to reach room temperature very slowly and was further stirred for 1.5 h. All the volatiles were removed in a vacuum, and the residue was heated at 100°C under reduced pressure for 2 h. 20 mL of chlorotrimethylsilane were then added, and the suspension was refluxed for 1.5 h. Afterward the volatiles were evaporated under reduced pressure, and the solid was washed with pentane (2×10 mL). The desired $^{68}\text{ZnCl}_2$ was obtained as a white solid in 92% yield (0.930 g).

Synthesis of $^{68}\text{Zn}(\text{C}_5\text{Me}_5)_2$. A mixture of $^{68}\text{ZnCl}_2$ (0.550 g, 3.95 mmol) and KC_5Me_5 (1.37 g, 7.91 mmol) was suspended in 30 mL of THF and stirred for 2.5 h at room temperature. The solvent was evaporated under a vacuum, and the residue was extracted with pentane (40 mL) yielding $^{68}\text{Zn}(\text{C}_5\text{Me}_5)_2$ as a pale yellow solid (0.804 g, 62%), with ^1H and $^{13}\text{C}\{^1\text{H}\}$ NMR spectra identical to those of $\text{Zn}(\text{C}_5\text{Me}_5)_2$.^{21b}

Compound 1, $\text{Zn}_2(\eta^5\text{-C}_5\text{Me}_5)_2$. To a mixture of $\text{Zn}(\text{C}_5\text{Me}_5)_2$ (3.0 g, 8.9 mmol), ZnCl_2 (1.21 g, 8.9 mmol), and KH (0.72 g, 17.9 mmol) was added THF (70 mL). The suspension was stirred at room temperature for 50 min, and afterward all the volatiles were removed in vacuo. The residue was dissolved in pentane (120 mL), and the solution was filtered off. A white crystalline solid was obtained by evaporation of the pentane under reduced pressure. The compound can be crystallized from pentane or from diethyl ether solutions, at -20°C . It sublimates at temperatures between 70 and 80°C , 10^{-3} mbar. Despite its thermal stability, due to its extreme reactivity toward oxygen and water it is best kept at -20°C under an argon atmosphere. Yield: 2.08 g (58%). ^1H NMR (500 MHz, C_6D_6): δ 2.02 (s, CH_3). $^{13}\text{C}\{^1\text{H}\}$ NMR (125 MHz, C_6D_6): δ 10.0 (C_5Me_5), 108.8 (C_5Me_5).^{21b} Compound 1 can be also obtained following the same synthetic procedure but using CaH_2 as the reducing agent: To a mixture of $\text{Zn}(\text{C}_5\text{Me}_5)_2$ (1.0 g, 3.0 mmol), ZnCl_2 (0.40 g, 3.0 mmol) and CaH_2 (0.12 g, 3.0 mmol) was added THF (40 mL), and the mixture stirred for 2 h and 45 min. After workup **1** was isolated in 48% yield (0.540 g). HRMS m/z calculated for $\text{C}_{20}\text{H}_{30}\text{Zn}_2$ (M^+): 400.0899, found: 400.0904.

The labeled $^{68}\text{Zn}_2(\text{C}_5\text{Me}_5)_2$ dimetalloocene was obtained following the same synthetic route described for **1** but using $^{68}\text{Zn}(\text{C}_5\text{Me}_5)_2$ and $^{68}\text{ZnCl}_2$ as the starting materials. The ^1H and $^{13}\text{C}\{^1\text{H}\}$ NMR spectra are identical to those observed for **1**. HRMS m/z calculated for $\text{C}_{20}\text{H}_{30}^{68}\text{Zn}_2$ (M^+): 406.0783, found: 406.0848.

Compound 2, $\text{Zn}_2(\eta^5\text{-C}_5\text{Me}_4\text{Et})_2$: A mixture of $\text{KC}_5\text{Me}_4\text{Et}$ (3.10 g, 36.6 mmol) and ZnCl_2 (2.5 g, 18.6 mmol) was dissolved in THF (50 mL) and stirred for 4 h at room temperature. The solvent was evaporated in vacuo, and the residue was extracted with pentane (3×15 mL). After removing the pentane, **2** was obtained as a yellow oil in ca. 70% yield. Crystals of **2** suitable for X-ray studies were obtained by slow evaporation of its pentane solutions at -20°C or by low-temperature (-80°C) crystallization of concentrated pentane solutions. Compound **2** is also highly reactive toward O_2 and H_2O and has lower thermal stability than **1** decomposing slowly, particularly in the form of a solid,

Table 3. X-ray Data for **1**, **2**, and **5**

| | 1 | 2 | 5 |
|---|---|---|---|
| formula | $\text{C}_{20}\text{H}_{30}\text{Zn}_2$ | $\text{C}_{22}\text{H}_{34}\text{Zn}_2$ | $\text{C}_{22}\text{H}_{46}\text{N}_2\text{O}_2\text{Zn}_2$ |
| fw | 401.18 | 429.23 | 501.35 |
| crystal system | triclinic | triclinic | triclinic |
| space group | $P\bar{1}$ | $P\bar{1}$ | $P\bar{1}$ |
| a , Å | 6.9329(3) | 7.0428(4) | 8.1668(6) |
| b , Å | 10.8831(5) | 10.3194(6) | 8.1758(6) |
| c , Å | 13.8384(7) | 14.8036(9) | 10.7877(1) |
| α , deg | 109.777(1) | 86.446(2) | 67.755(2) |
| β , deg | 101.603(1) | 89.191(2) | 77.755(3) |
| γ , deg | 94.201(1) | 76.599(2) | 75.470(2) |
| V , Å ³ | 951.09(8) | 1044.58(11) | 639.83(9) |
| Z | 2 | 2 | 1 |
| D_{calcd} , Mg m^{-3} | 1.401 | 1.365 | 1.301 |
| μ , mm^{-1} | 2.517 | 2.296 | 1.892 |
| θ_{max} , deg | 29.31 | 30.51 | 30.53 |
| temp, K | 173(2) | 100(2) | 173(2) |
| no. reflns collected | 11 466 | 26 394 | 10 512 |
| no. reflns used | 4662 | 6267 | 3864 |
| no. of param | 209 | 227 | 145 |
| R1 [$I > 2\sigma(I)$] ^a | 0.0310 | 0.0326 | 0.0383 |
| wR2 (all data) ^a | 0.0759 | 0.0833 | 0.1035 |
| GOF | 0.988 | 1.037 | 1.079 |

at temperatures between 0 and 20°C . It is advisable to store it at -20°C (or below) under argon. ^1H NMR (500 MHz, C_6D_6): δ 0.90 (t, $J_{\text{HH}} = 7.5$ Hz, 3H, $\text{CH}_3\text{-Et}$), 1.89 (s, 6H, $\text{CH}_3\text{-Cp}$), 1.90 (s, 6H, $\text{CH}_3\text{-Cp}^*$), 2.24 (q, $J_{\text{HH}} = 7.5$ Hz, 2H, $\text{CH}_2\text{-Et}$). $^{13}\text{C}\{^1\text{H}\}$ NMR (125 MHz, C_6D_6): δ 10.5 (s, $\text{CH}_3\text{-Cp}$), 10.6 (s, $\text{CH}_3\text{-Cp}$), 16.1 (s, $\text{CH}_3\text{-Et}$), 19.5 (s, $\text{CH}_2\text{-Et}$), 108.3 (s, $\text{C}_q\text{-Cp}$), 112.6 (s, $\text{C}_q\text{-Cp}$), 114.2 (s, $\text{C}_q\text{-Cp}$). Yield: 70% (2.0 g).

Compound 5, $[\text{ZnEt}(\text{TEMPO})_2]$. To a mixture of $\text{Zn}(\text{C}_5\text{Me}_5)_2$ (335 mg, 1 mmol) and TEMPO (93 mg, 0.6 mmol) in diethyl ether (20 mL) at -10°C , ZnEt_2 (1 mL, 1 mmol) was added. The resultant mixture was stirred at -10°C for 1 h, and the solvent was removed in vacuo. The residue was extracted with pentane (20 mL) and crystallized from the same solvent yielding the organometallic compound **4a** and **5**. ^1H NMR (500 MHz, C_6D_6): δ 0.8 (q, $J_{\text{HH}} = 8$ Hz, 4H), 1.17 (s, 24H), 1.44 (m, 8H), 1.54 (t, $J_{\text{HH}} = 8$ Hz, 6H).

The half-sandwich compounds $(\eta^5\text{-C}_5\text{Me}_5)\text{ZnR}$ ($\text{R} = \text{Me}, \text{Et}, \text{Ph}, \text{Mes}$) and other related derivatives containing different cyclopentadienyl ligands will be reported separately.³⁰

Computational Details. The geometries of all calculated complexes were computed within the density functional theory at the B3LYP level.⁵⁷ For Zn_2R_2 ($\text{R} = \text{CH}_3, \text{CF}_3, \text{SiH}_3$, and CCH) the 6-311++G** basis set was used for all atoms. For Zn_2R_2 ($\text{R} = \text{C}_5\text{H}_5, \text{C}_6\text{H}_5$) the 6-311G* basis set was used. In all cases for the calculation of reaction energies single-point calculations using the 6-311++G** basis set were done on the previously optimized geometries. All the optimized structures were characterized as real minima by diagonalization of the analytically computed Hessian ($\text{Nimag} = 0$). All the calculations were performed using the Gaussian-98 or Gaussian-03 package.⁵⁸ The MO analysis has been performed on the optimized structures with the 6-311G** basis set using the AOMIX program.^{49,50} Figures and pictures of selected MO have been obtained using Molekel.⁵⁹

For the calculation of the bond dissociation energy of the Zn–Zn bond a fragment-oriented approach was adopted⁵⁴ in order to evaluate the dissociation energy of the zinc–zinc bond (BDE) in species of general formula Zn_2R_2 . Two different procedure routes were envisaged (Scheme 4). Primary, the BDE is calculated directly by subtracting the energies of the optimized binuclear complex and the two mononuclear fragments that are allowed to relax to their equilibrium geometries after

(57) (a) Becke, A. D. *J. Chem. Phys.* **1993**, *98*, 5648. (b) Lee, C.; Wang, Y.; Parr, R. G. *Phys. Rev. B* **1988**, *37*, 785.

(58) Frisch, M. J., et al. *Gaussian 03*, revision C.02; Gaussian, Inc.: Wallingford, CT, 2004.

(59) Portmann, S.; Lüthi, H. MOLEKEL: An Interactive Molecular Graphics Tool. *Chimia* **2000**, *54*, 766.

the metal–metal bond rupture, $D(\text{Zn}–\text{Zn})$. Alternatively, the BDE is calculated in two steps. In the first the energy needed for “snapping” the metal–metal bond, $E(\text{Zn}–\text{Zn})$, is computed and then, in the second step, the energy gained when the isolated fragments relax from the conformation taken up in the original molecules to their optimal ground-state structure, ER, is evaluated. Taking into account the importance of the basis set superposition error (BSSE) associated with metal–metal bond energy calculations, the second procedure was selected, since the BSSE can be computed directly using the counterpoise method.⁶⁰ The $E(\text{Zn}–\text{Zn})$ value was obtained by building the Zn_2R_2 molecule from two ZnR fragments that have the geometry they adopt in the complex.

X-ray Crystal Structure Analyses of 1, 2, and 5. A single crystal of each representative compound (colorless prism 1, colorless prism 2, and colorless block 5) of suitable size was mounted on a glass fiber using perfluoropolyether oil (FOMBLIN 140/13, Aldrich) in the cold N_2 stream of the a low-temperature device attachment. A summary of crystallographic data and structure refinement is reported in Table 3. Intensity data for 1 were collected on a Siemens SMART 1 K diffractometer CCD area detector, equipped with a graphite monochromator $\lambda(\text{Mo K}\alpha_1) = 0.71073 \text{ \AA}$ and an Oxford Cryosystem low-temperature device, whereas the data collections for complexes 2 and 5 were performed on a Bruker-AXS X8Kappa diffractometer APEX-II CCD area detector, equipped with a graphite monochromator $\text{Mo K}\alpha_1$ ($\lambda = 0.71703 \text{ \AA}$) and a Bruker Cryo-Flex low-temperature device. The data collection strategy used in all instances was phi and omega

scans with narrow frames. Instrument and crystal stability were evaluated from the measurement of equivalent reflections at different measuring times, and no decay was observed. The data were reduced (SAINT)⁶¹ and corrected for Lorentz and polarization effects, and a semiempirical absorption correction was applied (SADABS).⁶² The structure was solved by direct methods (SIR-2002)⁶³ and refined against all F^2 data by full-matrix least-squares techniques (SHELXTL-6.12)⁶⁴ minimizing $w[F_o^2 - F_c^2]^2$. All the non-hydrogen atoms were refined with anisotropic displacement parameters. The hydrogen atoms were included from calculated positions and refined as riding contributions with isotropic displacement parameters 1.5 (methyl groups) times those of their respective attached carbon atoms.

Acknowledgment. We thank Dr. Angel Justo (Instituto de Ciencias de Materiales, Sevilla) for X-ray powder diffraction analysis of Zn and ZnO samples. We are also grateful to the X-ray diffraction service of the Universidad Autónoma de Madrid and to Mr. César J. Pastor as responsible for this service, for X-ray data collection at $-170 \text{ }^\circ\text{C}$ employing $\text{Cu K}\alpha$ radiation. I.R. thanks the Ministry of Education for a research grant. D.d.R. thanks the sixth framework program of the EU for an MC-OIF fellowship. Financial support from the DGEIC (Project CTQ 2004-409/BQU, FEDER support) and from the Junta de Andalucía is gratefully acknowledged.

Supporting Information Available: X-ray crystallographic data (CIF files). Table with selected bond distances for Zn_2R_2 optimized complexes and figures with selected MOs. Complete ref 58. This material is available free of charge via the Internet at <http://pubs.acs.org>.

JA0668217

(60) Boys, S. F.; Bernardi, F. *Mol. Phys.* **1970**, *19*, 553.

(61) *SAINT 6.02*; BRUKER-AXS, Inc.: Madison, WI 53711-5373, USA, 1997–1999.

(62) Sheldrick, G. *SADABS*; Bruker AXS, Inc.: Madison, WI, USA, 1999.

(63) Burla, M. C.; Camalli, M.; Carrozzini, B.; Cascarano, G. L.; Giacovazzo, C.; Polidori, G.; Spagna R. *SIR2002: the program. J. Appl. Crystallogr.* **2003**, *36*, 103.

(64) *SHELXTL 6.14*; Bruker AXS, Inc.: Madison, WI, USA, 2000–2003.